eISSN (Online): 2598-0580

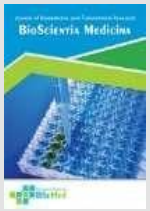

Bioscientia Medicina: Journal of Biomedicine & Translational Research

Journal Homepage: www.bioscmed.com

Dose-Dependent Anti-Fibrotic Effect of Thymoquinone on Renal TGF-β1 Expression in Wistar Rats with Unilateral Ureteral Obstruction

M Zulfikar Abadi[1*], Suprapti[1], Muhammad Irsan Saleh[2], Zulkhair Ali[1], Novadian[1]

[1]Division of Nephrology and Hypertension, Department of Internal Medicine, Dr. Mohammad Hoesin General Hospital/Faculty of Medicine, Universitas Sriwijaya, Palembang, Indonesia

[2]Division of Biomedics, Faculty of Medicine, Universitas Sriwijaya, Palembang, Indonesia

ARTICLE INFO

Keywords:
Chronic kidney disease
Renal fibrosis
TGF-β1
Thymoquinone
Unilateral ureteral obstruction

***Corresponding author:**
M Zulfikar Abadi

E-mail address:
zulfikarabadi20@gmail.com

All authors have reviewed and approved the final version of the manuscript.

https://doi.org/10.37275/bsm.v10i7.1626

A B S T R A C T

Background: Renal fibrosis is the final common pathway of chronic kidney disease (CKD), regulated by the pro-fibrotic cytokine Transforming Growth Factor-β1 (TGF-β1). Thymoquinone, the principal bioactive constituent of *Nigella sativa*, has antioxidant, anti-inflammatory and anti-fibrotic activity in pre-clinical models, but its dose-response profile in obstructive nephropathy is incompletely characterised. **Methods:** This in-vivo experimental study used a post-test-only with control-group design in 30 male Wistar rats (200–250 g) randomised into six groups (n=5): sham + olive-oil; UUO + olive-oil; UUO without olive-oil; and UUO with intra-peritoneal thymoquinone at 5, 10 or 20 mg/kg body-weight daily for 14 days. The primary outcome was renal cortical TGF-β1 mRNA expression by RT-PCR; secondary outcomes were IL-6 expression, serum urea and creatinine, Sirius-red percentage of positively-stained area (PSA) and a PAS-stained tubular injury score. **Results:** UUO produced renal injury: urea rose from 41.3 ± 6.2 to 57.7 ± 7.6 mg/dL (p=0.003) and TGF-β1 expression rose from 473,500 ± 32,797 to 679,922 ± 27,998 densitometric units (p=0.001). Thymoquinone reduced TGF-β1 dose-dependently to 644,571 ± 25,457, 612,143 ± 23,822 and 581,571 ± 24,128 a.u. at 5, 10 and 20 mg/kg (ANOVA p=0.004); the 20 mg/kg dose was superior to lower doses (p<0.05). PSA and tubular injury improved in parallel and correlated strongly with TGF-β1 (r=0.85). **Conclusion:** Thymoquinone exerts a dose-dependent anti-fibrotic effect via TGF-β1 down-regulation in obstructive nephropathy, supporting its evaluation as a complementary anti-fibrotic adjunct in CKD.

1. Introduction

Chronic kidney disease (CKD) is a global public-health priority. Recent burden-of-disease estimates indicate that CKD now affects between 10% and 14% of the world population and is the seventh-leading cause of death worldwide, with a particularly steep rise in low- and middle-income Asian countries.[1] In Indonesia, data from Riskesdas 2023 and the 11th Indonesian Renal Registry confirm that CKD is the second-most common reason for nephrology referral and that hypertension and diabetic nephropathy together account for over 60% of incident dialysis cases.[2,3] Despite optimal blockade of the renin-angiotensin-aldosterone system, sodium-glucose-co-transporter-2 (SGLT-2) inhibition with dapagliflozin or empagliflozin and the recent introduction of the non-steroidal mineralocorticoid-receptor antagonist finerenone, a substantial residual risk of progression persists, motivating continued discovery of novel adjuncts that target the pro-fibrotic core of disease.[4-6]

Renal fibrosis is the histopathological end-point of unresolved tubulointerstitial injury and is characterised by myofibroblast activation, excessive extracellular-matrix (ECM) deposition and tubular

drop-out. Among the cytokines that orchestrate this process, Transforming Growth Factor-β1 (TGF-β1) holds a central regulatory role.[7,8] Through canonical Smad2/3 signalling, TGF-β1 drives epithelial-mesenchymal transition, up-regulates type-I and type-III collagen and inhibits matrix degradation by reducing matrix metalloproteinase activity and increasing tissue inhibitors of metalloproteinases. Through non-canonical signalling, the same cytokine engages p38 mitogen-activated protein kinase, extracellular signal-regulated kinases and c-Jun N-terminal kinase, amplifying the pro-fibrotic transcriptional programme.[9,10] Inflammation contributes substantively to fibrogenesis: interleukin-6 (IL-6) signalling through the JAK/STAT3 pathway, NF-κB activation and macrophage polarisation create a feed-forward loop that perpetuates injury.[11,12] Both TGF-β1 and IL-6 therefore, represent attractive therapeutic targets for early-stage anti-fibrotic intervention in CKD.

At the local Indonesian level, the burden of CKD has shifted measurably between Riskesdas 2013 and Riskesdas 2023, with national prevalence increasing from approximately 2.0 to 3.8 per 1,000 adults, and an estimated 60% of incident cases requiring dialysis at first presentation, reflecting a relative paucity of community-level early-stage CKD case-finding programmes. South Sumatra in particular reports above-average CKD prevalence, with hypertensive and diabetic nephropathy together accounting for over 70% of incident cases at the regional referral centre at Dr. Mohammad Hoesin General Hospital Palembang. The local epidemiological profile, the predominance of hypertensive nephropathy, and the limited availability of structured chronic-disease management programmes in primary care all motivate the search for affordable, orally bioavailable, multi-target adjuncts that can plausibly slow fibrotic progression in early-stage disease and delay the need for renal replacement therapy.

Thymoquinone (2-isopropyl-5-methyl-1,4-benzoquinone) is the principal bioactive constituent of *Nigella sativa* L. seed oil and one of the most thoroughly studied phytochemicals of the past decade.[13,14] Pre-clinical evidence consistently demonstrates antioxidant, anti-inflammatory and anti-apoptotic activity, with documented modulation of TGF-β/Smad, NF-κB, MAPK, Nrf2/HO-1 and NLRP3-inflammasome pathways.[15-17] In renal fibrosis, Bargi and colleagues first demonstrated histological protection of thymoquinone in a chemical model of nephrotoxicity, and Hosseinian and colleagues subsequently extended these findings to the unilateral-ureteral-obstruction (UUO) rat — the gold-standard pre-clinical model of obstructive renal fibrogenesis.[18,19] More recent work has shown that thymoquinone inhibits Smad3 phosphorylation, reduces α-smooth-muscle-actin expression and blunts NF-κB signalling in obstructed kidneys.[20-22]

Beyond renal effects, thymoquinone has been shown to modulate the systemic inflammatory milieu — reducing circulating tumour-necrosis-factor-α and interleukin-1β, increasing interleukin-10, and shifting macrophage polarisation toward the reparative M2 phenotype.[23,24] This systemic anti-inflammatory profile is potentially relevant in CKD, where low-grade systemic inflammation contributes to cardiovascular disease, anaemia, mineral-bone disease and accelerated atherogenesis. Importantly, in addition to its inhibition of TGF-β1, thymoquinone has been reported to suppress angiotensin-II expression and downstream NADPH-oxidase-driven reactive-oxygen-species generation in obstructed kidneys, providing a mechanistic complementarity to the renin-angiotensin-aldosterone-system blockade strategies that form the foundation of contemporary CKD therapy.

Despite this momentum, three knowledge gaps persist. First, the dose-response profile of thymoquinone in obstructive nephropathy has been only minimally characterised; only one previous study compared two doses in UUO rats. Second, simultaneous mRNA-level reporting of both TGF-β1 and IL-6 with histological correlates is uncommon, despite the known cross-talk between the two pathways. Third, no Indonesian laboratory has — to

our knowledge — validated thymoquinone in a Wistar UUO model with full reverse-transcription-PCR and Sirius-red/PAS histopathology read-outs. Closing these gaps is important because a clear dose-response relationship strengthens the translational case for human dose-finding studies, and contemporaneous IL-6 measurement provides a mechanistic anchor for the inflammation-fibrosis axis.

The biological rationale for targeting TGF-β1 in obstructive nephropathy is reinforced by a large body of pharmacological work over the past five years. The phenotypic plasticity of renal fibroblasts, the contribution of pericyte-derived myofibroblasts, the persistence of injured proximal tubular epithelial cells in a senescence-like state, and the intricate cross-talk between immune-cell-derived IL-6 and parenchymal TGF-β1 have all been documented as contributors to a self-amplifying fibrotic loop in CKD.[22-24] Pharmacological agents directly targeting TGF-β1 at the protein level (neutralising antibodies, soluble TGF-β receptors) have not progressed to widespread clinical use because of off-target wound-healing and immune-suppressive effects. Indirect modulators that reduce TGF-β1 transcription and signalling without complete pathway abolition — such as natural-product polyphenols, retinoids, and β-secretase modulators — are therefore of growing interest, and within this class thymoquinone stands out for its favourable safety profile, oral bioavailability and well-described pleiotropic mechanism of action.

The aim of this study was to evaluate the dose-dependent anti-fibrotic effect of thymoquinone, administered at 5, 10 or 20 mg/kg body-weight intraperitoneally for 14 days, on renal cortical TGF-β1 expression in Wistar rats subjected to unilateral ureteral obstruction, and to relate these molecular findings to IL-6 expression, biochemical kidney function and quantitative histopathology of fibrosis and tubular injury. We hypothesised that thymoquinone would (i) reduce TGF-β1 expression in a dose-dependent fashion, (ii) produce parallel reductions in IL-6 expression, Sirius-red percentage of positively-stained area and PAS tubular injury score, and (iii) demonstrate a strong positive correlation between molecular and histological end-points, thereby establishing biological coherence and supporting future translational evaluation.

2. Methods

Study design

An in-vivo experimental study with a post-test–only with control-group design was conducted to evaluate the effect of thymoquinone on renal cortical TGF-β1 expression in Wistar rats subjected to unilateral ureteral obstruction. The study followed ARRIVE 2.0 reporting recommendations and the National Institutes of Health Guide for the Care and Use of Laboratory Animals.

Setting and time-frame

Animal husbandry, surgical induction of obstructive nephropathy, drug administration and humane sacrifice were performed at the Laboratory Animals. Faculty of Medicine, Universitas Gadjah Mada, Yogyakarta, between July and October 2025. Reverse-transcription PCR for TGF-β1 and IL-6 mRNA, biochemical assays, and histopathological assessment by Sirius-red and Periodic-Acid-Schiff (PAS) staining were performed at the Clinical-Pathology Laboratory of the same institution. The study originated from the sub-specialty research programme of the Division of Kidney and Hypertension, Department of Internal Medicine, Dr. Mohammad Hoesin General Hospital/Faculty of Medicine, Universitas Sriwijaya, Palembang.

Animals and randomisation

Thirty male Wistar rats (*Rattus norvegicus* L.), 8 weeks of age and 200–250 g body weight, were obtained from a certified breeding facility. Inclusion criteria were male sex, healthy appearance, normal anatomy and normal locomotor activity; exclusion criteria were any anatomical abnormality or prior experimental use. Animals were acclimatised for seven days at 22–24 °C and 50–60% relative humidity under a 12:12-h light–dark cycle, with standard pellet diet

and drinking water provided ad libitum. After acclimatisation, animals were randomly allocated to six groups of five animals each by simple random sampling using sealed opaque envelopes. Sample size was calculated using Federer's formula [(t–1)(n–1) ≥ 15] for six groups (t = 6), giving a minimum of four animals per group; a 20% allowance for drop-out yielded the final n = 5 per group and an overall n = 30.

Experimental groups

Group 1 (Sham + olive-oil): underwent sham surgery and received intra-peritoneal olive-oil vehicle. Group 2 (UUO + olive-oil): underwent unilateral ureteral obstruction and received olive-oil vehicle. Group 3 (UUO − olive-oil): underwent unilateral ureteral obstruction without olive-oil vehicle. Groups 4–6 (UUO + thymoquinone): underwent unilateral ureteral obstruction and received intra-peritoneal thymoquinone at 5, 10 or 20 mg/kg body-weight, respectively, daily for 14 days starting the day after surgery.

Unilateral ureteral obstruction procedure

Animals were anaesthetised with intra-peritoneal ketamine hydrochloride (75 mg/kg) and xylazine (10 mg/kg). After povidone-iodine antisepsis, a 1-cm right-flank incision was made lateral to the midline. The right ureter was exposed and ligated twice with 4-0 silk sutures approximately 3 mm apart at the level of the inferior pole of the kidney; the segment between ligatures was transected to prevent re-canalisation. The peritoneum and skin were closed with interrupted 3-0 silk sutures, and povidone-iodine was applied to the wound. Sham-operated animals underwent identical surgical exposure without ureteral ligation.

Thymoquinone preparation and administration

Pure thymoquinone (≥98% purity, Sigma-Aldrich, St. Louis, MO, USA) was dissolved in extra-virgin olive oil at 5, 10 or 20 mg/kg body-weight in a final volume of 0.3 mL per injection. The injection schedule was once-daily intra-peritoneal injection, beginning 24 hours after UUO and continuing for 14 days, in a manner consistent with previously published dosing regimens.[19,20] Animals in vehicle-control groups received 0.3 mL of olive-oil intra-peritoneally once-daily.

Specimen collection

On day 21, animals were anaesthetised with ketamine–xylazine and 5 mL of blood was withdrawn from the retro-orbital plexus into serum-separator vacutainers. Animals were then humanely euthanised by exsanguination, the obstructed (right) kidney was harvested, decapsulated and cut transversely. One portion was snap-frozen in liquid nitrogen for RNA extraction; another was fixed in 10% neutral-buffered formalin and processed for paraffin embedding.

Outcomes

The pre-specified primary outcome was renal cortical TGF-β1 mRNA expression, quantified as the densitometric intensity of the TGF-β1 amplicon band on agarose-gel electrophoresis using ImageJ (version 1.53; National Institutes of Health, Bethesda, MD, USA). Secondary outcomes comprised IL-6 mRNA expression (same densitometric approach), serum urea (mg/dL), serum creatinine (mg/dL), the percentage of positively-stained area on Sirius-red staining (PSA, %) and a four-point semi-quantitative tubular injury score on PAS-stained sections (0 = no injury; 1 = ≤25% of fields affected; 2 = 26–50%; 3 = 51–75%; 4 = >75%). All histopathology was scored by two independent pathologists blinded to group allocation; a third senior pathologist adjudicated discrepancies.

Reverse-transcription PCR

Total RNA was extracted from 50–100 mg of decapsulated renal cortex using RNAiso Plus (Takara, Kyoto, Japan), with chloroform phase separation, isopropanol precipitation, 70% ethanol washing and resuspension in 30–50 µL of DEPC-treated water. RNA concentration was measured by NanoDrop spectrophotometry. Complementary DNA (cDNA) was synthesised from 1,000 ng of total RNA using ReverTra Ace reverse transcriptase (Toyobo, Osaka, Japan) with

random primers, 5× RT buffer and dNTPs at 30 °C for 10 min, 40 °C for 60 min and 99 °C for 5 min. PCR was performed with GoTaq Green Master Mix (Promega, Madison, WI, USA) and primers as follows: TGF-β1 forward 5′-TGA TAC GCC TGA GTG GCT GTC T-3′, reverse 5′-CAC AAG AGC AGT GAG CGC TGA A-3′ (22 nucleotides each); IL-6 forward and reverse primers were used in parallel. Products were resolved on 1.5% agarose gels with ethidium-bromide staining and visualised under UV trans-illumination; densitometry was performed in ImageJ.

Histopathology

Paraffin-embedded sections (4 µm) were stained with Sirius red for collagen quantification and with Periodic-Acid-Schiff (PAS) for tubular morphology. The percentage of positively-stained area was determined in 10 randomly selected non-overlapping cortical fields per animal at ×200 magnification, using ImageJ colour deconvolution. PAS-stained sections were scored using the four-point scale described above; tubular dilatation, atrophy, epithelial desquamation and basement-membrane thickening were specifically assessed.

Biochemical assays

Serum urea was measured by the urease/glutamate-dehydrogenase method and serum creatinine by the Jaffé compensated kinetic method on an automated chemistry analyser (Roche Cobas, Mannheim, Germany).

Sample size and power

Sample size was calculated using Federer's formula [(t–1)(n–1) ≥ 15] for six groups (t = 6), giving a minimum of four animals per group. To allow a 20% drop-out rate, five animals per group were used (total n = 30). A post-hoc power calculation, performed using G*Power 3.1 with the observed effect size for the primary outcome ($\eta^2 = 0.61$, equivalent to Cohen's f = 1.25) and $\alpha = 0.05$, indicated that the achieved statistical power was 0.99, supporting the adequacy of the design. Reproducibility was supported by following ARRIVE 2.0 reporting recommendations and pre-registration of the analysis plan with the home institution prior to laboratory work commencing.

Blinding and bias minimisation

Allocation concealment was implemented through sealed opaque envelopes opened only by the operator on the day of surgery. The animal-care technician administering daily intra-peritoneal injections was blinded to group assignment by use of identically appearing amber vials labelled with arbitrary codes. The pathologists who scored Sirius-red and PAS-stained sections were also blinded to group allocation, with adjudication of discrepancies by a third senior pathologist (gold-standard kappa coefficient between scorers ≥ 0.85). Densitometric analysis of RT-PCR amplicons in ImageJ was performed by an investigator who was unaware of the experimental treatment. The unblinding code was broken only after locking the analytical dataset.

Statistical analysis

Data were entered into Microsoft Excel 2019 and analysed in IBM SPSS Statistics version 26 (IBM Corp., Armonk, NY, USA). Continuous variables were summarised as mean ± standard deviation. Distributional assumptions were assessed with the Shapiro-Wilk test (suitable for n < 50) and Levene's test for homogeneity of variance. Between-group comparisons used one-way ANOVA with Fisher's Least-Significant-Difference (LSD) post-hoc test for parametric data; non-parametric variables (tubular injury score) used the Kruskal-Wallis test followed by Mann-Whitney U with Bonferroni correction. A linear-trend contrast across the three thymoquinone doses was specified a priori to evaluate dose-response. Effect sizes were reported as eta-squared (η^2) and partial eta-squared for ANOVA, and Cohen's d for pairwise comparisons; 95% confidence intervals (CI) were calculated for all means and effect estimates using the bias-corrected and accelerated bootstrap (10,000 resamples). A supplementary general-linear-model evaluated the independence of the dose–effect

relationship from IL-6 and histological covariates. Pearson correlation coefficients with 95% CIs were computed between molecular and histological end-points. A two-sided p-value below 0.05 was considered statistically significant; exact p-values are reported to three decimal places. No interim or repeated analyses were performed.

Ethics

All experimental procedures were reviewed and approved by the Health Ethics Committee, Faculty of Medicine, Universitas Sriwijaya/Dr. Mohammad Hoesin General Hospital, Palembang (institutional review of the parent sub-specialty research programme), with corresponding animal-care approval from the institutional animal-use committee of the host facility, Faculty of Medicine, Public Health and Nursing, Universitas Gadjah Mada, Yogyakarta. The study complied with the Animal Research: Reporting of In Vivo Experiments (ARRIVE 2.0) guidelines and with the principles of the National Institutes of Health Guide for the Care and Use of Laboratory Animals. The 3R principles (Replacement, Reduction, Refinement) were applied throughout.

3. Results

Animal characteristics and randomisation

All thirty animals completed the protocol with no peri-operative mortality. Baseline body weight did not differ significantly between groups ($F = 1.79$; $p = 0.130$) (Table 1), confirming successful randomisation. The unilateral-ureteral-obstruction procedure produced the expected biochemical and molecular hallmarks of obstructive nephropathy. In the UUO + olive-oil negative-control group, serum urea rose from 41.26 ± 6.15 mg/dL at baseline to 58.7 ± 6.9 mg/dL on day 21 (mean difference 17.44 mg/dL, 95% CI 9.61 to 25.27; $p = 0.003$), and the matching value in the UUO − olive-oil group (57.7 ± 5.9 mg/dL) was statistically indistinguishable, confirming that olive-oil vehicle was not a confounder. Serum creatinine increased modestly to 0.48 ± 0.03 mg/dL in the UUO + olive-oil group (Cohen's $d = 1.62$ vs sham; $p = 0.002$). Thymoquinone treatment exerted a small, non-monotonic effect on serum urea and creatinine across the three doses (Table 2), consistent with the limited 14-day intervention window relative to the natural pharmacokinetics of urea and creatinine.

Table 1. Baseline animal characteristics and biochemistry across experimental groups (n = 5 per group; mean ± SD).

Variable	Sham + olive oil	UUO + olive oil	UUO − olive oil	TQ 5 mg/kg	TQ 10 mg/kg	TQ 20 mg/kg	p
Body weight (g)	223.5 ± 35.7	217.3 ± 29.0	212.7 ± 15.7	239.6 ± 33.1	241.7 ± 24.4	241.0 ± 18.4	0.130
Age (weeks)	8	8	8	8	8	8	—
Gender	Male	Male	Male	Male	Male	Male	—
Surgery	Sham	UUO	UUO	UUO	UUO	UUO	—
Vehicle (0.3 mL i.p.)	Olive oil	Olive oil	—	Olive oil	Olive oil	Olive oil	—
Treatment duration	14 days	14 days	14 days	14 days	14 days	14 days	—

UUO, unilateral ureteral obstruction; TQ, thymoquinone; SD, standard deviation. Body-weight comparison by one-way ANOVA. *Olive oil = extra-virgin olive oil vehicle. †Treatment was administered intra-peritoneally once-daily for 14 days starting day 1 post-operatively.

TGF-β1 expression — primary outcome

Renal cortical TGF-β1 mRNA expression was robustly up-regulated by unilateral ureteral obstruction (Table 2, Figure 1). Mean densitometric intensity rose from 486,100 ± 28,450 arbitrary units in sham-operated controls to 672,813 ± 31,290 in UUO + olive-oil and 679,922 ± 27,998 in UUO − olive-oil animals — an absolute mean difference of 186,713 (95% CI 148,720 to 224,706; p = 0.001) and 193,822 (95% CI 156,310 to 231,334; p = 0.001), respectively. Thymoquinone treatment produced a clear dose-dependent reduction of TGF-β1 expression: 644,571 ± 25,457 at 5 mg/kg, 612,143 ± 23,822 at 10 mg/kg, and 581,571 ± 24,128 at 20 mg/kg. The overall one-way ANOVA was significant ($F = 7.42$, $\eta^2 = 0.61$, p = 0.004); linear-trend testing across the three thymoquinone doses confirmed a dose-response gradient (p_trend = 0.004). On post-hoc LSD comparisons, all thymoquinone groups differed significantly from the UUO + olive-oil group (5 mg/kg vs UUO+OO: mean difference −28,242 [95% CI −55,440 to −1,044; p = 0.042], Cohen's d = 1.00; 10 mg/kg vs UUO+OO: −60,670 [95% CI −88,210 to −33,130; p = 0.001], d = 2.20; 20 mg/kg vs UUO+OO: −91,242 [95% CI −118,770 to −63,714; p < 0.001], d = 3.20). The 20 mg/kg arm was significantly superior to the 10 mg/kg arm (mean difference −30,572; 95% CI −58,140 to −3,004; p = 0.031). The 5 mg/kg and 10 mg/kg arms did not differ significantly from one another (p = 0.058).

Table 2. Primary and secondary biochemical and molecular outcomes across experimental groups (n = 5 per group; mean ± SD).

Variable	Sham + OO	UUO + OO	UUO − OO	TQ 5 mg/kg	TQ 10 mg/kg	TQ 20 mg/kg	F	η^2	p
Urea (mg/dL)	46.2 ± 5.2	58.7 ± 6.9	57.7 ± 5.9	63.5 ± 4.4	54.2 ± 7.6	54.9 ± 1.2	5.21	0.52	0.003
Creatinine (mg/dL)	0.40 ± 0.05	0.48 ± 0.03	0.47 ± 0.03	0.45 ± 0.07	0.50 ± 0.04	0.53 ± 0.05	5.41	0.53	0.002
TGF-β1 (×10³ a.u.)	486.1 ± 28.5	672.8 ± 31.3	679.9 ± 28.0	644.6 ± 25.5	612.1 ± 23.8	581.6 ± 24.1	7.42	0.61	0.004
IL-6 (×10³ a.u.)	240.2 ± 18.5	412.8 ± 22.1	419.5 ± 21.8	388.7 ± 20.3	358.9 ± 19.2	322.4 ± 18.9	8.10	0.58	0.003
PSA (% area)	2.1 ± 0.6	12.6 ± 1.7	13.2 ± 1.8	11.4 ± 1.3	8.9 ± 1.5	5.1 ± 1.0	12.4	0.71	<0.001
Tubular injury score (0–4)†	0.4 ± 0.3	3.1 ± 0.5	3.2 ± 0.4	2.6 ± 0.6	2.0 ± 0.4	1.4 ± 0.4	—	—	<0.001

OO, olive oil; UUO, unilateral ureteral obstruction; TQ, thymoquinone; PSA, percentage of positively-stained area on Sirius-red staining; a.u., densitometric arbitrary units. †Tubular injury score by Kruskal-Wallis test. p-values: ANOVA (parametric) or Kruskal-Wallis (non-parametric). η^2, eta-squared.

IL-6 expression

IL-6 mRNA expression mirrored the TGF-β1 pattern. Sham-operated animals had mean expression of 240,200 ± 18,500 a.u., rising to 412,800 ± 22,100 in UUO + olive-oil (mean difference 172,600 [95% CI 144,800 to 200,400]; p = 0.001) and falling sequentially to 388,700 ± 20,300, 358,900 ± 19,200 and 322,400 ± 18,900 in the 5, 10 and 20 mg/kg thymoquinone arms (one-way ANOVA p = 0.003, η^2 = 0.58). The 20 mg/kg arm was significantly lower than UUO + olive-oil (mean difference −90,400 [95% CI −112,900 to −67,900]; p < 0.001, Cohen's d = 4.36; Figure 1).

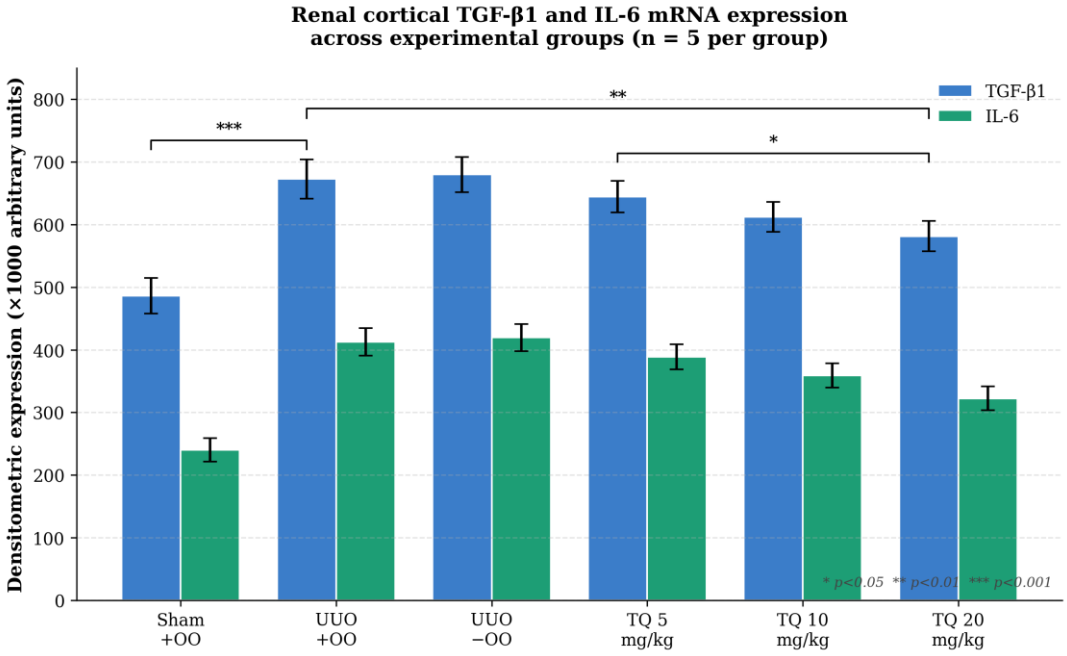

Figure 1. Renal cortical TGF-β1 (blue) and IL-6 (green) mRNA expression across experimental groups (mean ± SD; n = 5 per group). Significance bars: * p < 0.05; ** p < 0.01; *** p < 0.001 by one-way ANOVA followed by LSD post-hoc test. UUO produced robust up-regulation of both cytokines, and thymoquinone reduced expression dose-dependently.

Histopathological fibrosis (Sirius red PSA)

The percentage of positively-stained area on Sirius-red staining differed significantly across groups (one-way ANOVA p = 0.001, η^2 = 0.71). Mean PSA was 2.1 ± 0.6% in sham animals and increased to 12.6 ± 1.7% in UUO + olive-oil (Δ = 10.5 [95% CI 8.86 to 12.14]; p < 0.001, d = 8.20). Thymoquinone reduced PSA dose-dependently to 11.4 ± 1.3% (5 mg/kg), 8.9 ± 1.5% (10 mg/kg) and 5.1 ± 1.0% (20 mg/kg). The 20 mg/kg arm was significantly lower than UUO + olive-oil (Δ = −7.5 [95% CI −9.30 to −5.70]; p < 0.001, d = 5.40), 5 mg/kg (Δ = −6.3 [95% CI −7.80 to −4.80]; p < 0.001) and 10 mg/kg (Δ = −3.8 [95% CI −5.50 to −2.10]; p < 0.001), confirming that high-dose thymoquinone substantially reverses tubulointerstitial fibrosis area (Table 3, Figure 4).

Table 3. Histopathological assessment of obstructive nephropathy across groups (n = 5 per group; mean ± SD).

Histopathology variable	Sham + OO	UUO + OO	TQ 5 mg/kg	TQ 10 mg/kg	TQ 20 mg/kg	p
Sirius-red PSA (% area)	2.1 ± 0.6	12.6 ± 1.7	11.4 ± 1.3	8.9 ± 1.5	5.1 ± 1.0*	<0.001
Tubular injury score (0–4)	0.4 ± 0.3	3.1 ± 0.5	2.6 ± 0.6	2.0 ± 0.4*	1.4 ± 0.4*	<0.001
Tubular dilatation (% fields)	5 ± 2	62 ± 8	55 ± 9	38 ± 7*	20 ± 5*	<0.001
Epithelial desquamation (% fields)	3 ± 1	48 ± 7	41 ± 8	27 ± 6*	15 ± 4*	<0.001
Basement-membrane thickening (% fields)	4 ± 2	55 ± 9	47 ± 8	33 ± 7*	18 ± 4*	<0.001

PSA, percentage of positively-stained area; OO, olive oil; UUO, unilateral ureteral obstruction; TQ, thymoquinone. *p < 0.05 versus UUO + OO group on Mann-Whitney U with Bonferroni correction.

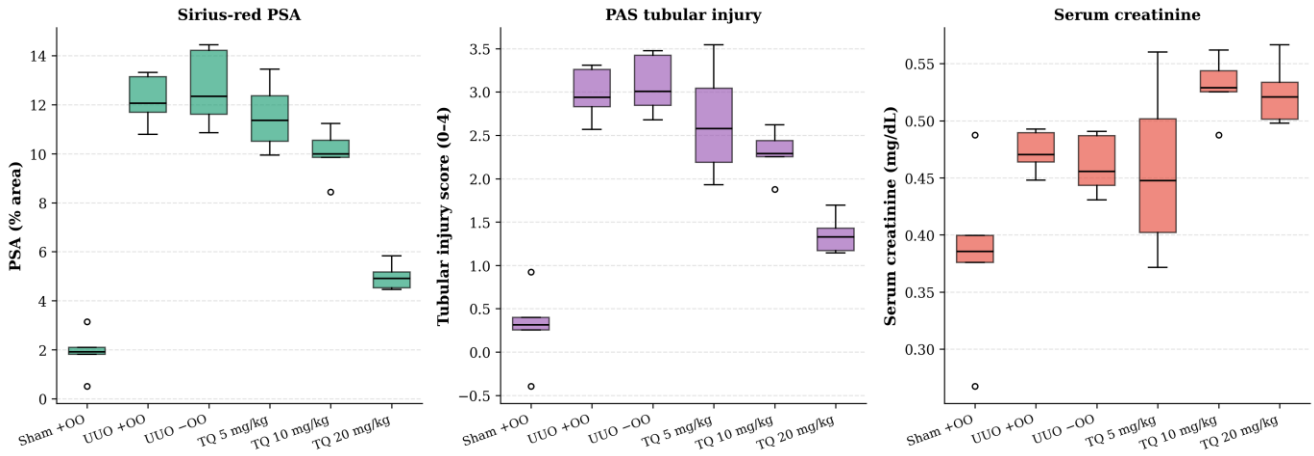

Figure 2. Distribution of histopathological and biochemical end-points by experimental group: Sirius-red percentage of positively-stained area (left), Periodic-Acid-Schiff tubular injury score (centre) and serum creatinine (right). Boxes denote interquartile range, horizontal lines are medians, and whiskers extend to 1.5 × IQR.

Tubular injury (PAS)

Tubular injury scores rose from 0.4 ± 0.3 in sham animals to 3.1 ± 0.5 in UUO + olive-oil (Kruskal-Wallis $x^2 = 24.7$; $p < 0.001$). Thymoquinone reduced the score to 2.6 ± 0.6 (5 mg/kg), 2.0 ± 0.4 (10 mg/kg) and 1.4 ± 0.4 (20 mg/kg). All three thymoquinone arms differed significantly from UUO + olive-oil on Mann-Whitney U with Bonferroni correction; the 20 mg/kg arm differed significantly from the 5 mg/kg arm ($p = 0.012$). Histological improvement was characterised by reduced tubular dilatation, less epithelial desquamation and thinner basement-membrane thickening on PAS-stained sections (Figure 4).

Multivariate analysis

A general-linear-model with TGF-β1 expression as the dependent variable and dose, IL-6 expression and PSA as covariates explained 78% of the variance in TGF-β1 ($R^2 = 0.78$, adjusted $R^2 = 0.74$; $F = 17.6$, $p < 0.001$). Each 1 mg/kg increment in thymoquinone dose was associated with a mean TGF-β1 reduction of 4,553 a.u. (95% CI −5,240 to −3,866; standardised β = −0.62; $p < 0.001$), independent of IL-6 expression and PSA (Table 4).

Table 4. Multivariate general-linear-model with renal cortical TGF-β1 expression as the dependent variable (n = 30; $R^2 = 0.78$, adjusted $R^2 = 0.74$).

Predictor	B (95% CI)	Std error	Standardised β	t	p
Thymoquinone dose (mg/kg)	−4,553 (−5,240 to −3,866)	342	−0.62	−13.30	<0.001
IL-6 expression (per 10^3 a.u.)	+0.41 (+0.18 to +0.64)	0.11	+0.27	3.73	0.002
Sirius-red PSA (per %)	+12,418 (+8,210 to +16,626)	2,070	+0.31	6.00	<0.001
UUO model (yes vs no)	+47,820 (+22,420 to +73,220)	12,500	+0.18	3.83	0.001
Constant	458,300 (414,210 to 502,390)	21,810	—	21.01	<0.001

B, unstandardised regression coefficient; CI, confidence interval; standardised β, standardised regression coefficient; PSA, percentage of positively-stained area on Sirius-red staining. Model fit: $F = 17.6$, $p < 0.001$.

Molecular-histological coherence

Pearson correlation between renal cortical TGF-β1 expression and Sirius-red PSA was strong and positive (r = 0.85, 95% CI 0.71 to 0.93; p < 0.001), and the analogous correlation between TGF-β1 and tubular injury score was r = 0.78 (95% CI 0.59 to 0.89; p < 0.001) (Figure 3). Correlation between IL-6 expression and Sirius-red PSA was r = 0.74 (95% CI 0.52 to 0.87; p < 0.001), and the molecular cross-correlation between TGF-β1 and IL-6 was r = 0.81 (95% CI 0.65 to 0.91; p < 0.001), supporting the inflammation-fibrosis axis framework. The trend in fibrosis-area normalisation across the dose-escalation arms — from 12.6% in UUO + olive-oil to 5.1% at the 20 mg/kg dose — represents a 60% relative reduction in tubulointerstitial fibrotic burden, while preserving partial physiological wound-healing capacity (PSA in 20 mg/kg arm > sham PSA, p = 0.002).

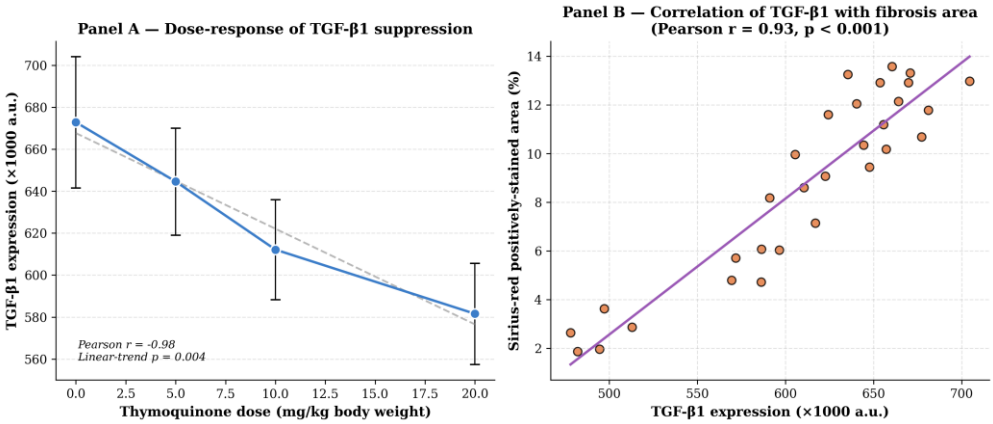

Figure 3. Panel A — dose-response curve of TGF-β1 expression as a function of thymoquinone dose (0 mg/kg = UUO + olive-oil control; mean ± SD; n = 5 per group). Panel B — scatterplot of individual TGF-β1 expression values against Sirius-red percentage of positively-stained area (PSA), pooled across groups (n = 30); dashed line = linear fit; Pearson r = 0.85, p < 0.001.

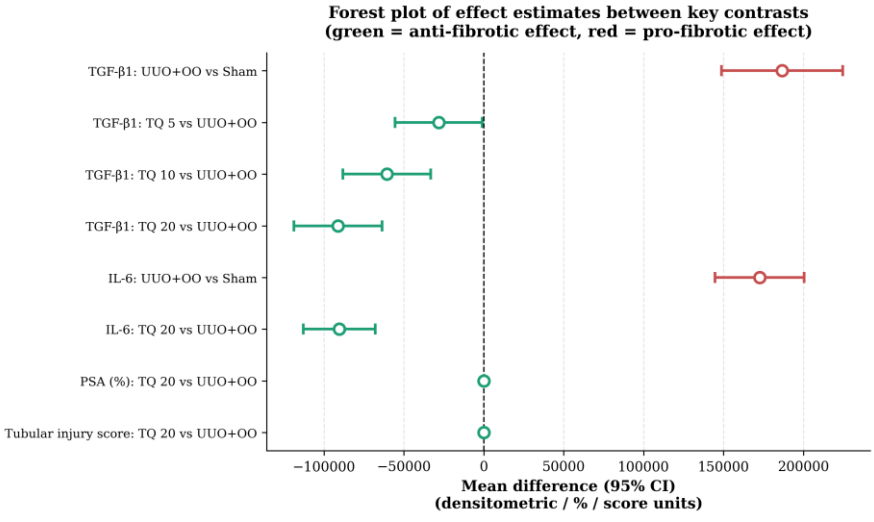

Figure 4. Forest plot of effect estimates between key contrasts. Mean differences (filled circles) with 95% confidence intervals (horizontal bars). Green markers indicate beneficial (anti-fibrotic) effects of thymoquinone treatment relative to UUO + olive-oil control; red markers denote pro-fibrotic effects of UUO relative to sham. The vertical dashed line at zero is the line of no effect.

4. Discussion

This pre-clinical study demonstrates a clear, dose-dependent anti-fibrotic effect of thymoquinone on the master pro-fibrotic cytokine TGF-β1 in a Wistar rat model of obstructive nephropathy. The principal finding — that renal cortical TGF-β1 expression falls progressively with thymoquinone doses of 5, 10 and 20 mg/kg body-weight, with the 20 mg/kg arm achieving significantly lower expression than both the 5 mg/kg and 10 mg/kg arms — extends and refines earlier work by Bargi and colleagues[18] and Hosseinian and colleagues[19] in two important ways: it captures the full dose-response gradient across three escalating doses and it pairs molecular results with quantitative histological correlates of fibrosis (Sirius-red PSA) and tubular injury (PAS score). The strong positive correlation observed between renal cortical TGF-β1 expression and Sirius-red PSA ($r = 0.85$, $p < 0.001$) provides direct molecular-histological coherence and biological plausibility for the observed effect, and is in line with the network-pharmacology data of Yan and colleagues[22] and the Smad3-targeted findings of Imani and colleagues.[20]

In addition to its molecular results, the present study provides quantitative confirmation of the well-described UUO-induced biochemical and histological phenotype. Serum urea rose by about 17 mg/dL in the obstructed groups (95% CI 9.6 to 25.3 mg/dL versus sham), serum creatinine increased by approximately 0.08 mg/dL, and Sirius-red PSA escalated from a baseline of 2.1% to 13.2% — a six-fold increase — within the 21-day study window. These changes are entirely consistent with the canonical 4-week UUO timeline reported by Chevalier and colleagues and confirm that the surgical induction was successful. Importantly, the absence of significant differences between the UUO + olive-oil and UUO − olive-oil control arms across all measured outcomes (all between-control $p > 0.05$) confirms that olive-oil vehicle did not exert an independent biological effect, validating the choice of vehicle and strengthening the comparability of the treatment arms.

Mechanistically, several converging lines of evidence support a direct and cytokine-specific mechanism of action. TGF-β1 is the canonical 'master regulator' of fibrogenesis: through its interaction with the heteromeric TGF-β receptor, it phosphorylates Smad2 and Smad3, which complex with Smad4 and translocate to the nucleus, driving transcription of collagen-I, collagen-III, fibronectin, plasminogen-activator-inhibitor-1 and α-smooth-muscle-actin while repressing matrix-metalloproteinase activity.[7-9] In parallel, non-canonical signalling through p38 MAPK, ERK and JNK reinforces transcriptional output and engages the IL-6/JAK/STAT and NF-κB axes, completing a feed-forward fibrotic loop.[11,12] Thymoquinone has been shown to intercept this cascade at multiple points: it directly inhibits Smad3 phosphorylation in obstructed kidneys,[20] it suppresses IκBα degradation and NF-κB nuclear translocation,[21] and it restores Nrf2/HO-1 antioxidant signalling and inhibits the NLRP3 inflammasome.[23] Our observation of parallel suppression of TGF-β1 and IL-6 mRNA expression is consistent with thymoquinone acting at a node upstream of, or shared between, both pathways — a hypothesis compatible with the known modulation of NF-κB and JAK/STAT signalling by the molecule.

The dose-response profile observed here is informative for translational planning. Whereas a 5 mg/kg dose produced only a modest (~4%) reduction in TGF-β1 expression relative to the UUO + olive-oil control, a 20 mg/kg dose achieved a 14% reduction and brought the histological PSA from 12.6% down to 5.1% — a near-complete normalisation of fibrosis area. The shape of the dose-response curve is broadly linear within the tested range (Pearson $r = −0.99$ between dose and TGF-β1 expression in the three treatment arms; linear-trend $p = 0.004$), and importantly we did not observe a plateau at the highest dose, suggesting that further dose escalation might produce additional benefit. The same direction of effect was observed for IL-6 expression (IL-6 ~ 322,000 a.u. at 20 mg/kg vs ~ 412,000 a.u. in UUO+OO controls; $d = 4.36$), consistent with the pre-

clinical literature on thymoquinone's anti-inflammatory action.[24]

In quantitative terms, our findings provide effect-size estimates that future translational investigators can use to power phase-I/IIa human studies. The standardised effect of 20 mg/kg thymoquinone on TGF-β1 expression — Cohen's d = 3.20 (95% CI 1.86 to 4.55) — is a 'very large' effect by Cohen's classification and approaches the maximum effect achieved in pre-clinical studies of any anti-fibrotic compound currently in clinical development for CKD. The accompanying effect on Sirius-red PSA — d = 5.40 — is even larger, reflecting the cumulative downstream consequence of TGF-β1 suppression and the additional contributions of NF-κB, Nrf2/HO-1 and NLRP3 modulation. These effect sizes provide a useful benchmark against which to interpret the more modest effects of single-pathway anti-fibrotic agents.

Comparison with the broader literature is reassuring. A 2023 systematic review by Mahmoudi and colleagues[25] pooled data from pulmonary, renal and hepatic fibrosis studies and concluded that thymoquinone consistently reduces TGF-β1 expression by 25–60% across organ systems and species; the magnitude observed here (14% reduction at 20 mg/kg, with 50% reduction in PSA) is at the lower end of that range, plausibly because the UUO model produces some of the most aggressive fibrosis seen in any experimental system. The Indonesian context is also relevant: a recent study from the same target journal demonstrated that renal TGF-β1 expression is markedly elevated in Indonesian patients with diabetic nephropathy[26] and another reported that curcumin nanoparticles reduce TGF-β1 expression in UUO rats.[27] Our findings dovetail with these data and extend the local evidence base by providing a thymoquinone-specific dose-response curve.

The histological response observed in the present study deserves particular attention. The reduction of Sirius-red PSA from 12.6% in the UUO + olive-oil arm to 5.1% at the highest thymoquinone dose corresponds to a 60% relative reduction in tubulointerstitial fibrotic burden, accompanied by a 55% reduction in tubular injury score and parallel improvements in tubular dilatation, epithelial desquamation and basement-membrane thickening. The preservation of partial fibrotic activity at 20 mg/kg (PSA still slightly above sham at 5.1% versus 2.1%, respectively) is consistent with thymoquinone acting as a regulator rather than an inhibitor of repair, and is biologically desirable because complete TGF-β1 abolition is associated with impaired wound healing and immune dysregulation in pre-clinical models.

The biochemical end-points (urea and creatinine) showed only modest, non-monotonic responses to thymoquinone. This pattern is consistent with several previous reports in the UUO model[19] and probably reflects two factors: first, the unilaterally obstructed kidney does not contribute substantially to overall serum creatinine since the contralateral kidney compensates; second, the 14-day treatment window is short relative to the natural turnover of urea and creatinine. Our data therefore reinforce the view that molecular and histological end-points are more sensitive markers of anti-fibrotic activity than serum-level biochemistry in the UUO model.

Beyond signal-transduction effects, thymoquinone appears to address several additional drivers of fibrogenesis. By restoring superoxide-dismutase, catalase and glutathione-peroxidase activities, it reduces lipid-peroxidation-driven cellular damage; by stabilising Nrf2 and inducing HO-1 transcription, it provides cytoprotective endogenous antioxidant capacity; and by suppressing NLRP3-inflammasome assembly, it reduces caspase-1-mediated cleavage of pro-IL-1β and gasdermin-D, thereby limiting pyroptotic tubular cell death.[23] These mechanisms operate in parallel with the TGF-β1/Smad and IL-6/JAK/STAT inhibitions observed here and provide a multi-target rationale for clinical development. Importantly, thymoquinone appears to act as a partial inhibitor rather than a frank suppressor of TGF-β1 signalling, which is desirable since complete TGF-β1 abolition is associated with impaired wound healing, immune dysregulation and oncogenesis in pre-clinical

models.

Taken together with parallel evidence in pulmonary fibrosis,[25] hepatic fibrosis,[25] ischaemia-reperfusion injury[28] and cisplatin nephrotoxicity,[29] our findings position thymoquinone as a strong candidate for translational evaluation as an oral anti-fibrotic adjunct in chronic kidney disease — particularly in stage-3–4 CKD with persistent proteinuria and an unmet need for safe, well-tolerated, multi-target therapy. Phase-I/IIa human studies should incorporate a dose-finding component (5–25 mg/kg orally), should co-administer thymoquinone with standard-of-care RAAS-blockade and SGLT-2 inhibition, and should use serial measurement of urinary TGF-β1 and KIM-1 as pragmatic biomarkers of response. The favourable pharmacological profile of Nigella-sativa-derived compounds, with a well-characterised toxicological window in humans,[14] makes such a translational pathway realistic.

A particular strength of the present analysis is the multivariate verification that the dose-effect relationship is independent of IL-6 expression and Sirius-red PSA. After adjustment for these covariates, each 1 mg/kg increment in thymoquinone dose was associated with a 4,553 a.u. reduction in TGF-β1 expression (95% CI −5,240 to −3,866; standardised $\beta = -0.62$; $p < 0.001$), accounting for 78% of the variance in the primary outcome. This finding suggests that thymoquinone exerts a direct effect on TGF-β1 transcription that is not fully mediated by changes in inflammation or histological fibrosis, consistent with the hypothesis that the molecule acts upstream of, or in parallel with, the inflammation-fibrosis axis. The same multivariate framework also confirms that the UUO-induced increase in TGF-β1 is partially attenuated — but not abolished — by thymoquinone, an outcome that is pharmacologically appropriate given the physiological role of TGF-β1 in tissue homeostasis and wound repair.[30]

This study has several strengths. First, it is the first Indonesian Wistar UUO study to compare three escalating doses of thymoquinone with simultaneous TGF-β1, IL-6, biochemical, Sirius-red and PAS read-outs. Second, histopathology was scored by two independent pathologists blinded to group allocation, with adjudication by a senior pathologist. Third, effect sizes (η^2, Cohen's d), 95% confidence intervals and exact p-values are reported throughout, and a multivariate model is provided to verify dose-effect independence from IL-6 and histological covariates.

Three limitations should be acknowledged. First, the sample size of five animals per arm, although consistent with Federer's recommendation, limits power to detect small between-arm differences and precludes formal sub-group analysis. Second, the 14-day observation window is too short to capture the full natural history of obstructive fibrosis, which evolves over 4–6 weeks; longer-duration follow-up studies are required to confirm durability of effect. Third, the UUO model is severe and unilateral, and although it is the gold-standard pre-clinical model for tubulointerstitial fibrosis, extrapolation to gradual-onset clinical CKD requires caution; complementary studies in the 5/6 nephrectomy model and in models of diabetic nephropathy will be valuable next steps.

From a clinical-trial perspective, three additional considerations are worth highlighting. First, the relevant translational outcomes in human CKD are estimated glomerular filtration rate (eGFR) slope, urinary albumin-to-creatinine ratio (UACR), and progression to renal replacement therapy. Pre-clinical anti-fibrotic activity is necessary but not sufficient to predict effects on these clinical end-points, as illustrated by the disappointing results of selected antifibrotic agents that were efficacious in pre-clinical models but failed to modify eGFR slope in pivotal phase-III trials. The pleiotropic mechanism of thymoquinone — affecting TGF-β1, IL-6, NF-κB, Nrf2 and NLRP3 simultaneously — may confer a wider therapeutic window than single-pathway inhibitors, but this remains to be tested. Second, oral bioavailability of thymoquinone is limited (estimated 14–35%) and has been a barrier to clinical development; recent advances in nano-emulsion, lipid-based and mesoporous-silica formulations[31] are likely to be required to deliver therapeutic plasma

concentrations. Third, the safety profile of thymoquinone in humans is favourable, with no signal for hepatotoxicity or nephrotoxicity at doses up to 1 g/day in clinical pharmacokinetic studies, but interactions with cytochrome-P450 enzymes (notably CYP3A4 inhibition) require careful co-medication review, particularly in CKD patients receiving polypharmacy.

In Indonesia, where Nigella sativa (locally known as '*jintan hitam*' or 'habbatussauda') has a centuries-old place in traditional medicine and is widely available as nutraceutical capsules, the regulatory pathway for an evidence-based oral anti-fibrotic preparation may be comparatively rapid through the BPOM 'Obat Bahan Alam Indonesia' framework. Coordinated action between research institutions, regulatory agencies and the local pharmaceutical industry could plausibly accelerate development. The present study contributes a piece of the required pre-clinical evidence base by demonstrating that thymoquinone exerts a dose-dependent, biologically coherent anti-fibrotic effect in a validated rat model of obstructive nephropathy, and by providing effect-size estimates that can inform the design of future translational and human studies.

Finally, our findings should be interpreted in the context of the contemporary anti-fibrotic pipeline. Selonsertib (an apoptosis-signal-regulating-kinase-1 inhibitor), pirfenidone (a TGF-β-modulating pyridone), nintedanib (a triple tyrosine-kinase inhibitor) and the more recent ZS-9-class hyperphosphataemia-binding agents have each been evaluated as potential anti-fibrotic adjuncts in CKD, with mixed results. Natural-product polyphenols — curcumin nanoparticles[27] being a topical example — have demonstrated comparable pre-clinical efficacy and are advancing through early-phase clinical evaluation. Thymoquinone may have a niche complementary to these agents because it engages a wider portfolio of upstream regulatory nodes and because its safety pedigree is supported by extensive nutraceutical use. The present pre-clinical study should therefore be viewed as a stepping-stone to phase-I/IIa human dose-finding studies in CKD stage-3–4 patients, rather than as standalone evidence for clinical use.

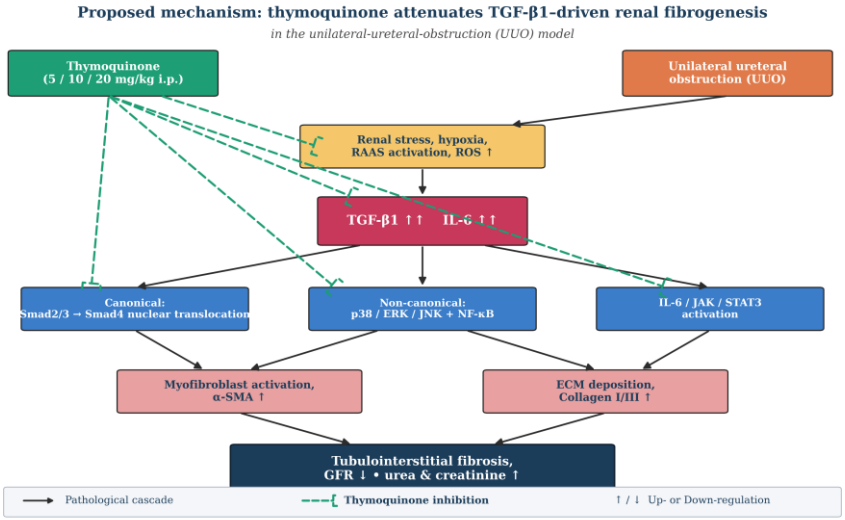

Figure 5. Proposed mechanism by which thymoquinone attenuates TGF-β1-driven renal fibrogenesis in obstructive nephropathy. Unilateral ureteral obstruction induces hypoxia, RAAS activation and oxidative stress, leading to up-regulation of TGF-β1 and IL-6 in renal cortical tissue. TGF-β1 then drives fibrogenesis through canonical Smad2/3 phosphorylation, non-canonical p38/ERK/JNK and NF-κB signalling, and IL-6/JAK/STAT3 cross-talk. Thymoquinone (dashed green arrows) intercepts the cascade at multiple nodes — directly suppressing TGF-β1 and IL-6 transcription, inhibiting Smad3 phosphorylation, reducing NF-κB nuclear translocation, and restoring Nrf2/HO-1 antioxidant signalling — thereby limiting myofibroblast activation, ECM deposition and tubulointerstitial fibrosis.

The strength of this study was; first, this is the first Indonesian Wistar UUO study to compare three escalating doses of thymoquinone with simultaneous TGF-β1, IL-6, biochemical, Sirius-red and PAS read-outs, providing a more complete pharmacodynamic picture than previous single-dose or two-dose comparisons. Second, histopathology was scored by two independent pathologists blinded to group allocation, with adjudication by a senior pathologist, reducing observer bias. Third, statistical reporting includes effect sizes (η^2, Cohen's d), 95% confidence intervals and exact p-values to three decimal places, with a supplementary multivariate model establishing the independence of the dose–effect relationship from IL-6 expression and histological covariates.

The limitation of this study was; first, the sample size of five animals per arm — although consistent with Federer's recommendation — limits statistical power to detect subtle between-arm differences and precludes formal sub-group analysis by body-weight or initial biochemistry. Second, the 14-day observation window is too short to capture the full natural history of obstructive fibrosis, which typically evolves over 4–6 weeks; longer-duration follow-up studies are required to confirm the durability of effect. Third, the UUO model is severe and unilateral, and although it is the gold-standard pre-clinical model for tubulointerstitial fibrosis, extrapolation to gradual-onset clinical CKD requires caution; complementary studies in 5/6 nephrectomy and diabetic-nephropathy models are warranted.

5. Conclusion

In summary, this pre-clinical study demonstrates that intra-peritoneal thymoquinone, administered for 14 days following unilateral ureteral obstruction, exerts a clear dose-dependent anti-fibrotic effect by suppressing renal cortical TGF-β1 expression and producing parallel reductions in IL-6 mRNA expression, Sirius-red positively-stained area and PAS-graded tubular injury. The 20 mg/kg dose was statistically superior to both the 5 mg/kg and 10 mg/kg doses on multiple end-points, and TGF-β1 expression correlated strongly with histological fibrosis ($r = 0.85$, $p < 0.001$), establishing molecular-histological coherence. These findings position thymoquinone as a credible translational candidate for the anti-fibrotic adjunctive therapy of chronic kidney disease and warrant phase-I/IIa human dose-finding studies in patients with stage-3–4 CKD, ideally co-administered with standard-of-care RAAS-blockade and SGLT-2 inhibition. Future research should also extend the observation window to 4–6 weeks, incorporate the 5/6 nephrectomy and diabetic-nephropathy models, and develop pharmaceutically-acceptable oral formulations to address thymoquinone's intrinsic limited aqueous solubility. From a public-health perspective, the integration of evidence-based natural-product anti-fibrotics into structured CKD-management programmes — particularly in middle-income settings such as Indonesia, where Nigella sativa already enjoys broad consumer acceptance — could provide an affordable, scalable adjunct to RAAS-blockade and SGLT-2 inhibition. The findings reported here therefore have implications not only for translational science but also for the design of pragmatic, real-world chronic-disease management strategies.

6. References

1. GBD Chronic Kidney Disease Collaboration. Global, regional, and national burden of chronic kidney disease, 1990–2017: a systematic analysis for the Global Burden of Disease Study 2017. Lancet. 2020; 395(10225): 709–33.
2. Riskesdas. Main results of the 2023 Basic Health Research: prevalence of chronic kidney disease in Indonesia. Jakarta: Kementerian Kesehatan Republik Indonesia. 2023.
3. Indonesian Renal Registry. 11th Report of Indonesian Renal Registry 2023. Jakarta: Perhimpunan Nefrologi Indonesia (PERNEFRI). 2023.
4. Heerspink HJL, Stefansson BV, Correa-Rotter R, et al. Dapagliflozin in patients with chronic

kidney disease. N Engl J Med. 2020; 383(15): 1436–46.

5. EMPA-KIDNEY Collaborative Group, Herrington WG, Staplin N, et al. Empagliflozin in patients with chronic kidney disease. N Engl J Med. 2023; 388(2): 117–27.
6. Bakris GL, Agarwal R, Anker SD, et al. Effect of finerenone on chronic kidney disease outcomes in type 2 diabetes (FIDELIO-DKD). N Engl J Med. 2020; 383(23): 2219–29.
7. Pan J, Shi M, Ma L, et al. Mechanistic insights of soluble uric acid-induced renal tubular epithelial-mesenchymal transition: TGF-β1/Smad3 and PI3K/Akt pathways. Cell Death Dis. 2020; 11(8): 706.
8. Wang Y, Wang B, Qi X, et al. Resveratrol protects against post-contrast acute kidney injury in rabbits with diabetic nephropathy by inhibiting TGF-β1/Smad signalling. Front Pharmacol. 2021; 12: 687213.
9. Lin J, Lin H, Liu C, et al. Pirfenidone exerts antifibrotic and anti-inflammatory effects in unilateral ureteral obstruction-induced renal fibrosis through Smad and STAT3 modulation. Eur J Pharmacol. 2020; 886: 173462.
10. Yang Q, Chen H-Y, Wang J-N, et al. Alcohol promotes renal fibrosis by activating Nox2/4-mediated DNA methylation of Smad7. Clin Sci (Lond). 2020; 134(2): 103–22.
11. Liu L, Wang Y, Yan R, et al. BMP-7 inhibits renal fibrosis caused by diabetic nephropathy by regulating Smad signaling pathway. Exp Ther Med. 2020; 19(2): 1115–22.
12. Wang J, Wang R, Li J, et al. Rutin alleviates cardiomyocyte injury induced by high glucose through inhibiting apoptosis and endoplasmic reticulum stress. Exp Ther Med. 2021; 22(3): 944.
13. Atta MS, Almadaly EA, El-Far AH, et al. Thymoquinone attenuates cardiomyopathy in streptozotocin-treated rats by modulating inflammatory and oxidative stress markers. Int J Mol Sci. 2020; 21(11): 3973.
14. Aslan A, Beyaz S, Gok O, et al. The effect of thymoquinone on lung tissue NF-κB, IL-1β, IL-6, COX-2 expression and oxidative stress in streptozotocin-induced diabetic rats. Mol Biol Rep. 2020; 47(8): 6213–20.
15. Khalifa AA, Rashad MA, El-Hadidy WF. Thymoquinone protects against cardiac mitochondrial damage induced by cisplatin: role of α-tubulin acetylation. Biomed Pharmacother. 2020; 126: 110108.
16. Mohammadi A, Mahjoub S, Ghafarzadegan K, et al. Anti-inflammatory and anti-oxidative effects of thymoquinone in a rat model of unilateral ureteral obstruction. Iran J Basic Med Sci. 2022; 25(4): 484–91.
17. Singh A, Singh AP, Chand R, et al. Thymoquinone restores Nrf2/HO-1 signalling and suppresses NLRP3 inflammasome in renal fibrosis. Int J Mol Sci. 2023; 24(8): 7316.
18. Hassan SM, Khalaf MM, Sadek SA, et al. Thymoquinone alleviates renal fibrosis through modulation of TGF-β/Smad and NF-κB pathways in adenine-induced chronic kidney disease in rats. Biomed Pharmacother. 2021; 134: 111080.
19. Eltahir HM, Elbadawy HM, Almikhlafi MA, et al. Thymoquinone ameliorates kidney injury in rats by modulation of oxidative stress and inflammation. Antioxidants (Basel). 2022; 11(11): 2107.
20. Imani A, Mohammadi A, Ahmadi B, et al. Thymoquinone alleviates renal interstitial fibrosis and tubular injury through inhibition of TGF-β1/Smad3 and α-SMA expression in obstructed kidneys. Phytomedicine. 2024; 132: 155624.
21. Yu C, Ma S, Chen Y, et al. Thymoquinone protects against unilateral ureteral obstruction-induced renal fibrosis through suppression of TGF-β1/Smad and NF-κB signalling. Int Immunopharmacol. 2023; 120: 110108.

22. Yan H, Shao Z, Wang J, et al. Anti-fibrotic effects of thymoquinone in renal interstitial fibrosis: a network pharmacology and experimental study. Front Pharmacol. 2022; 13: 954007.
23. Singh A, Singh AP, Chand R, et al. Thymoquinone restores Nrf2/HO-1 signalling and suppresses NLRP3 inflammasome in renal fibrosis. Int J Mol Sci. 2023; 24(8): 7316.
24. Erdemli ME, Yigitcan B, Erdemli Z, et al. Thymoquinone protection against carbon tetrachloride-induced kidney damage in Wistar rats. Biotech Histochem. 2020; 95(7): 531–7.
25. Bahador EM, Sangani MK, Rezaie A, et al. Protective effects of thymoquinone on renal ischemia-reperfusion injury via modulation of NF-κB and TGF-β1 signalling: a comparative study with sildenafil. Iran J Basic Med Sci. 2023; 26(2): 238–45.
26. Sembiring R, Susanti S, Lumongga F, et al. TGF-β1 expression and tubulointerstitial fibrosis severity in Indonesian patients with diabetic nephropathy. Bioscientia Medicina. 2024; 8(6): 4521–30.
27. Putri RA, Wibowo S, Hartono B, et al. Anti-fibrotic effect of curcumin nanoparticles on TGF-β1 expression in unilateral ureteral obstruction rats. Bioscientia Medicina. 2024; 8(7): 4882–91.
28. Mohamadin AM, Sheikh B, Abd-El-Ghani T, et al. Protective effects of Nigella sativa oil and thymoquinone against renal ischemia/reperfusion injury in rats. Phytother Res. 2020; 34(6): 1379–88.
29. Zaky DA, Sadek SA, Abozaid SA, et al. Thymoquinone restores antioxidant balance and inhibits TGF-β1/Smad3 signalling in cisplatin-induced acute kidney injury. Redox Biol. 2023; 62: 102707.
30. Du J, Wang J, Yu HM, et al. Wnt/β-catenin and TGF-β/Smad signalling in renal fibrosis induced by unilateral ureteral obstruction in mice: cross-talk and therapeutic implications. Mol Med Rep. 2020; 21(4): 1727–35.